Virtual Massive MIMO Beamforming Gains for 5G User Terminals

Muhammad Bilal Amin, Wolfgang Zirwas
Nokia Bell Labs
Munich, Germany
Email: {bilal.amin.ext, wolfgang.zirwas}@nokia.com

Martin Haardt
Communications Research Laboratory
Technische Universität Ilmenau, Germany
Email: martin.haardt@tu-ilmenau.de

***Abstract*—For future 5G systems significant performance benefits are expected from massive MIMO, especially in combination with tight inter-cell cooperation including joint-transmission using cooperative multi-point transmission. Most massive MIMO evaluations concentrate on the base station side with the goal to achieve high spectral efficiency by MU-MIMO or large coverage by strong beamforming gains. Especially for the, here interesting, below 6 GHz RF-bands user equipment (UE) sided analysis is typically limited to four or mostly eight antenna elements per UE, which can be justified by the limited space to place more antenna elements as well as the related UE complexity. At the same time, there would be many benefits from UE-sided beamforming, ranging from improved channel estimation and prediction accuracy, effective interference suppression up to coverage and spectral efficiency gains on the system level. In our previous work, we have already proposed virtual beamforming for channel estimation and prediction, while here we extend the concept to user data transmission over virtually generated beams. Virtual beamforming directly applied to user data can be very inefficient, a challenge we overcome by parallel transmission over a set of coded virtual beams.**

Keywords — massive MIMO; virtual beamforming; coded transmission

I. Introduction

The combination of a broader component carrier bandwidth, more spectrum, massive multiple-input multiple-output (MIMO) [1], and small cells to name a few are the technical components under consideration for future 5G radio systems to improve system performance metrics. Tight cooperation like joint-transmission coordinated multi-point (JT-CoMP) between adjacent sites is another cornerstone for a powerful inter-cell interference mitigation [2][3].

Massive MIMO transmission is the extension of conventional MIMO to an extremely large number of antenna elements, and is expected to improve spectral and energy efficiency, compared to LTE 8×8 MIMO, by spatial multiplexing of a comparably higher number of users (MU-MIMO). On the downlink (DL), these capacity or spectral efficiency gains based on JT-CoMP and massive MIMO both require an accurate knowledge of the channel state information at the transmitter (CSIT). For larger cooperation areas, a high number of relevant channel components (CCs) for all user equipments (UEs) have to be estimated as well as reported. A CC is defined as the effective channel from one transmit (Tx) to one receive (Rx) beam and relevant CCs are those that lie within a certain power window [4]. In practical systems, the CSIT is usually imperfect due to mobility and corresponding channel out-dating, which implies a mismatch between the actual and fed-back radio channels. Channel prediction can efficiently combat feedback delays for uplink reporting and therefore has been identified as one of the main enablers for JT-CoMP, especially for frequency division duplex (FDD) systems. Furthermore, large prediction horizons are a means for less frequent reports and correspondingly low reporting overhead [5] or for improved MIMO precoding, multi-user scheduling, and adaptive modulation [6].

Channel estimation and prediction have been investigated for a long time [7][8], and extremely low errors in terms of the normalized mean square error (NMSE) of the predicted channels and decent prediction horizons, have been reported for artificial radio channels, especially in the high signal-to-noise (SNR) region. In typical real world macro outdoor scenarios, the estimation quality degrades due to a high number of up to several hundreds of relevant multipath components (MPCs), being directly unobservable for a channel impulse response (CIR) with limited tap resolution. In addition the presence of diffuse scatterers, birth and death of MPCs, time-varying channel conditions (e.g., from moving objects), etc. make accurate prediction even more difficult.

For 5G systems, there is still the opportunity to devise more radical and new design options, addressing the above mentioned challenges. In our previous work, we presented in [9] the concept of virtual beamforming (VB), with the goal to generate effective radio channels with a very limited number of relevant MPCs, which are then easy to predict by any state-of-the-art predictor. For virtual beamforming, moving UEs store the spatial information over several locations and combine this knowledge to form a virtual antenna array with correspondingly large virtual antenna array aperture size, allowing for more narrow Rx-beams.

In urban macro non-line-of-sight (NLOS) scenarios, UE-sided beamforming might reduce the number of MPCs very effectively, due to the large angle of arrival (AoA) spread of a UE, surrounded by multiple scatterers. By pointing the very narrow beam in the direction of the last interaction point of the strongest MPCs, a high number of MPCs and diffuse scatterers impinging from angles of arrival other than the main beam lobe will be filtered out. By employing *virtual beamforming* at the UE using, for example, 32 virtual antenna elements, it

978-1-5090-1701-0/16/$31.00 ©2016 IEEE

was shown in [9] and [4] that the low rank channel can be predicted for approximately 0.4λ with 10 dB lower NMSE for channel prediction as compared to that of the same SISO channel without virtual beamforming.

In FDD systems, after the UE estimates or predicts the channel, it is fed-back to the transmitter for efficient precoding and data transmission. This CSI reporting benefits again from VB, as it reduces the information content of the radio channel or in other words the channel fluctuations over time and frequency. While being very effective, VB leaves the important question, '*how should one design the overall system for data transmission?*' Reporting the virtually beamformed channel components provides CSI information only for the limited spatial subspace containing the relevant MPCs in the direction of the narrow virtual beam lobe. Assuming different user data are transmitted at every time slot, i.e,. without virtual beamforming, any MU-MIMO or CoMP precoding would fail due to mismatch to the reported radio channel.

One option would be to perform channel estimation/prediction at the UE multiple times over the full azimuth space of 360° and to combine all the spatial subspaces to obtain the full single-input single-output (SISO) CSI information over 360°. This has still the benefit of higher predictability per subspace but the final overall gain might be low, if there is any at all. The reason is that it will add up many small estimation errors and poses some issues for estimation complexity. The most challenging is that the virtual beams would overlap, hence capturing some MPCs twice and some MPCs would be captured with a higher receive power as compared to the others due to the shape of the conventional beams. In addition, side-lobes would cause interference to the main beam in the adjacent subsection. Trying to avoid these challenges led to the idea to reuse the same virtually beamformed radio channels not only for channel estimation/prediction, but also for user data transmission. This would minimize any mismatch between reported CSI and that being used, e.g., for the MU-MIMO user data transmissions.

For UEs with arrays consisting of physical, instead of virtual antenna elements, one can directly reuse the same beam pattern for data transmission. However, in the case of virtual antennas, such a solution will lead to very inefficient resource usage, as the very same data symbols have to be retransmitted for several time instants. To get the same, or at least similar, efficiency for virtual as compared to physical antenna arrays, we propose multiplexing of multiple data streams using mutually orthogonal codes of the same length as the virtual antenna array. This scheme of coded multiplexing of user data is the main focus of this paper, especially the quite specific interdependencies of codes and shape of the virtual beam patterns will be derived and analysed.

For 5G, the benefits of user data transmission over virtually beamformed channel components might be quite far reaching. The ability of UEs to form large virtual antenna arrays, despite limited implementation complexity for only one to few physical antennas and RF chains, can be used, for example, to form very effective interference rejection combining (IRC) filters. This will help to effectively combat inter-cell or inter-cooperation area interferers, transferring into large spectral efficiency gains [3][10], thus this concept might become an important part of a novel 5G air interface.

The general concept of virtual beamforming and coded transmission over virtual beams is discussed in Section II. Section III details the scheme for a combination of physical and virtual antennas and Section IV lists our conclusions.

II. Orthogonally Coded Data Transmission over Virtual Beams

Virtual beamforming (VB) allows us to generate a (virtual) uniform linear array (ULA) at the UE, even if the UE has only a single physical antenna [11]. The movement of the UE in time is utilized by storing the $R \in \mathcal{N}$ adjacent receive (Rx) signal measurements, which can then be considered as the signals received at the various antenna element (AE) positions of an array. For a certain mobile speed the time difference between the measurements is related to the spacing between the adjacent virtual elements. A weighting vector, $\mathbf{w} = [w_1, \ldots, w_\omega, \ldots, w_R]^T \in \mathcal{C}^{R\times 1}$ can then be applied to these measurements to generate the beamformed channel.

The main challenge for multiplexing of user data by coded transmission over virtual beams is that at the UE, the code is inevitably coupled with the beam shape. Often orthogonal codes have values which change sign from one value to the next, e.g., $+1$ or -1 in Hadamard codes. Such codes can result in a complete reversal of the phase shift between adjacent antenna elements, which results in undesired beam shapes and loss of gain as shown in Figure 1a for an antenna spacing of $0.1\ \lambda$. Code 1, which is the first row of the Hadamard matrix of size 32 (all ones code) has a desirable beam shape with the look direction at 90°, whereas code 2, which is another row of the Hadamard matrix has no energy in any particular direction and cannot be used as beam for data transmission. One way to get around this problem is to use nearly orthogonal circular codes of the form,

$$\mathbf{c}_k = e^{-j2\pi k\mathbf{r}/R} \tag{1}$$

where, $k = 0, 1, \ldots, K$, with K being the total number of codes or coded virtual beams, $\mathbf{r} = [1, 2, \ldots, R]^{\mathrm{T}}$, and R being the total number of (virtual) AEs. These kind of circular codes can give us usable beams, which are still fully orthogonal to each other, at least at the transmitter side, as shown in Figure 1b. Hence, we will use circular codes for our user data multiplexing scheme.

A. User Data Multiplexing Using Two Orthogonal Codes

To explain the main idea, we first start with a very basic setup of a single antenna transmitter and a single antenna UE in an urban macro scenario. The UE moves on a straight line with a constant speed. The transmit symbols d_1 and d_2 are simultaneously transmitted repeatedly over R time slots, where R is the number of measurements that will be stored at the UE to create the virtual AEs. At each time slot, the transmit symbols are multiplied by the respective code bit from the

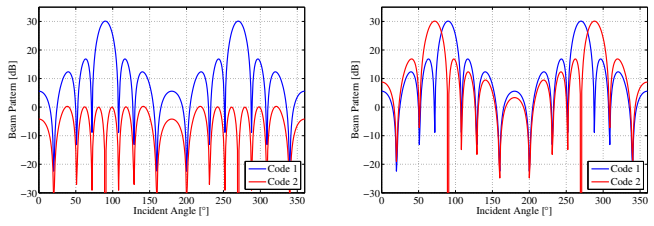

(a) Hadamard Code (b) Circular Code

Fig. 1: A comparison of beam patterns of two codes over a 32 element virtual array having a $\lambda/10$ spacing for different types of codes. Here, 0 dB represents the gain of an isotropic radiator.

code word of length R, corresponding to that transmit symbol. Here we consider a single sub-carrier. As in an OFDM system, the sub-carriers are orthogonal, hence they can carry separate transmit symbols and the following process can be separately applied to each of the sub-carriers. The transmission vector of length $R \times 1$ is then given as,

$$\mathbf{x} = \mathbf{c}_1 \circ \mathbf{d}_1 + \mathbf{c}_2 \circ \mathbf{d}_2. \tag{2}$$

Here, $\mathbf{d}_1 = d_1\mathbf{1}$ and $\mathbf{d}_2 = d_2\mathbf{1}$, where $\mathbf{1}$ is an all one vector of size R, and '$\circ$' is the Hadamard product of vectors. A simple schematic is provided in Figure 2, where the solid link is the actual location of the UE and the dashed lines show the past locations and stored measurements for the UE over time.

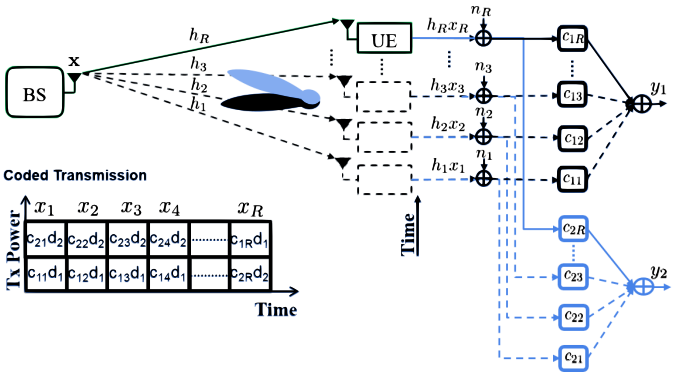

Fig. 2: A simple schematic of the coded data transmission and reception over virtual beams using two orthogonal codes

When the UE has moved for R time slots, we can combine the measurements from these locations to generate the virtual beams. As the codes are coupled with the beams, we use the codes themselves as the Rx-beamforming weights, hence $\mathbf{w}_1^{\mathrm{H}} = \mathbf{c}_1^{\mathrm{H}}$ and $\mathbf{w}_2^{\mathrm{H}} = \mathbf{c}_2^{\mathrm{H}}$ (Figure 1b). The receive beam signal for code 1 is given as,

$$\begin{aligned} y_1 &= \mathbf{c}_1^{\mathrm{H}}(\mathbf{h} \circ \mathbf{x} + \mathbf{n}) \\ &= \mathbf{c}_1^{\mathrm{H}}(\mathbf{h} \circ (\mathbf{c}_1 \circ \mathbf{d}_1 + \mathbf{c}_2 \circ \mathbf{d}_2) + \mathbf{n}) \\ &= \mathbf{c}_1^{\mathrm{H}}(\mathbf{h} \circ \mathbf{c}_1 \circ \mathbf{d}_1 + \mathbf{h} \circ \mathbf{c}_2 \circ \mathbf{d}_2 + \mathbf{n}) \\ &= \underbrace{\mathbf{c}_1^{\mathrm{H}}(\mathbf{h} \circ \mathbf{c}_1)}_{A} \circ \mathbf{c}_1^{\mathrm{H}}\mathbf{d}_1 + \underbrace{\mathbf{c}_1^{\mathrm{H}}(\mathbf{h} \circ \mathbf{c}_2)}_{XT_{12}} \circ \mathbf{c}_1^{\mathrm{H}}\mathbf{d}_2 + \underbrace{\mathbf{c}_1^{\mathrm{H}}\mathbf{n}}_{n_1}. \end{aligned} \tag{3}$$

Similarly the beam for the second code is given as,

$$\begin{aligned} y_2 &= \mathbf{c}_2^{\mathrm{H}}(\mathbf{h} \circ \mathbf{x} + \mathbf{n}) \\ &= \mathbf{c}_2^{\mathrm{H}}(\mathbf{h} \circ (\mathbf{c}_1 \circ \mathbf{d}_1 + \mathbf{c}_2 \circ \mathbf{d}_2) + \mathbf{n}) \\ &= \mathbf{c}_2^{\mathrm{H}}(\mathbf{h} \circ \mathbf{c}_1 \circ \mathbf{d}_1 + \mathbf{h} \circ \mathbf{c}_2 \circ \mathbf{d}_2 + \mathbf{n}) \\ &= \underbrace{\mathbf{c}_2^{\mathrm{H}}(\mathbf{h} \circ \mathbf{c}_1)}_{XT_{21}} \circ \mathbf{c}_2^{\mathrm{H}}\mathbf{d}_1 + \underbrace{\mathbf{c}_2^{\mathrm{H}}(\mathbf{h} \circ \mathbf{c}_2)}_{B} \circ \mathbf{c}_2^{\mathrm{H}}\mathbf{d}_2 + \underbrace{\mathbf{c}_2^{\mathrm{H}}\mathbf{n}}_{n_2} \end{aligned} \tag{4}$$

where A and B are the desired signal parts whereas XT_{12} and XT_{21} are the sum cross-talks, respectively, for data symbol vectors $\mathbf{d}_1$ and $\mathbf{d}_2$, and n_1 and n_2 are the corresponding noise samples.

We observe that the individual additional noise terms in each of the measurements are added together and amplified by the beamformer. For independent identically distributed (IID) noise values this leads to the same overall noise power as known for a physical antenna array. But, there is a penalty for the virtual versus the physical antenna array, as in the case of VB the Rx-power per time slot is limited to that of the physically available antenna elements. So for the user data multiplexing VB provides no or less beamforming signal to noise ratio (SNR) gains.

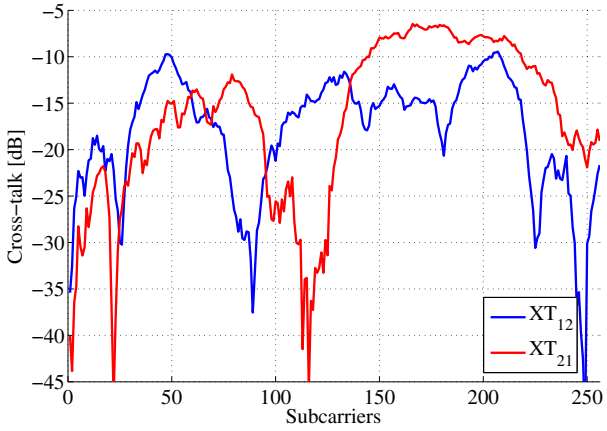

Fig. 3: Sum cross-talk XT_{12} and XT_{21} over sub-carriers using codes of length 32 for a measured channel.

The codes are orthogonal at the transmitter, but not at the UE receiver due to the time-varying nature of the channel. The sum cross-talks at the UE, XT_{12} and XT_{21}, can be calculated as the channel $\mathbf{h}$ is known at the UE side. In contrast the evolved NodeB (eNB) transmitter knows only the reported CSI per virtually beamformed radio channel and therefore cannot estimate this crosstalk.

If the cross-talk is low, we can formulate a system of linear equations which can be solved for the desired data symbols.

$$\begin{bmatrix} y_1 \\ y_2 \end{bmatrix} = \begin{bmatrix} A & XT_{12} \\ XT_{21} & B \end{bmatrix} \begin{bmatrix} d_1 \\ d_2 \end{bmatrix} + \begin{bmatrix} n_1 \\ n_2 \end{bmatrix}. \tag{5}$$

It can be solved for the desired symbols as,

$$\begin{bmatrix} d_1 \\ d_2 \end{bmatrix} = \begin{bmatrix} A & XT_{12} \\ XT_{21} & B \end{bmatrix}^{-1} \begin{bmatrix} y_1 \\ y_2 \end{bmatrix} - \begin{bmatrix} A & XT_{12} \\ XT_{21} & B \end{bmatrix}^{-1} \begin{bmatrix} n_1 \\ n_2 \end{bmatrix}. \tag{6}$$

Figure 3 shows the sum cross-talks for an urban macro measured channel with noise. A sum crosstalk of 0 dB means that the codes became non-orthogonal after passing through the channel and the undesired symbol in a certain receive beam has the same magnitude as the desired one. Hence, the desired data symbol cannot be resolved properly from the received signal. We can see that cross-talk below -15 dB or even -20 dB can be achieved, which would insure reliable communication over the coded virtual beams. The cross-talk goes above -10 dB for some of the sub-carriers but the coded beams might be adapted for different frequency sub-carriers to remain below the minimum cross-talk threshold all the time.

B. User Data Multiplexing Using Four Orthogonal Codes

We can now expand the same setup of a single antenna transmitter and a single antenna UE in an urban macro scenario to four orthogonal codes. Now we can transmit 4 data symbols over R time slots. This increases the efficiency from $2/R$ to $4/R$. We again consider a single sub-carrier. The transmission vector of length $R \times 1$ is given as,

$$\mathbf{x} = \mathbf{c}_1 \circ \mathbf{d}_1 + \mathbf{c}_2 \circ \mathbf{d}_2 + \mathbf{c}_3 \circ \mathbf{d}_3 + \mathbf{c}_4 \circ \mathbf{d}_4 \tag{7}$$

Here, $\mathbf{d}_1 = d_1\mathbf{1}$, $\mathbf{d}_2 = d_2\mathbf{1}$, $\mathbf{d}_3 = d_3\mathbf{1}$, and $\mathbf{d}_4 = d_4\mathbf{1}$ where $\mathbf{1}$ is an all one vector of size R.

Similar to the case with two codes, when the UE has moved for R time slots, we combine the measurements from these locations to generate the virtual beams. The receive beam signal for code 1 is given as,

$$\begin{aligned} y_1 &= \mathbf{c}_1^{\mathrm{H}}(\mathbf{h} \circ \mathbf{x} + \mathbf{n}) \\ &= \mathbf{c}_1^{\mathrm{H}}(\mathbf{h} \circ \mathbf{c}_1 \circ \mathbf{d}_1 + \mathbf{h} \circ \mathbf{c}_2 \circ \mathbf{d}_2 \\ &\quad + \mathbf{h} \circ \mathbf{c}_3 \circ \mathbf{d}_3 + \mathbf{h} \circ \mathbf{c}_4 \circ \mathbf{d}_4 + \mathbf{n}) \\ &= \underbrace{\mathbf{c}_1^{\mathrm{H}}(\mathbf{h} \circ \mathbf{c}_1)}_{A} \circ \mathbf{c}_1^{\mathrm{H}}\mathbf{d}_1 + \underbrace{\mathbf{c}_1^{\mathrm{H}}(\mathbf{h} \circ \mathbf{c}_2)}_{XT_{12}} \circ \mathbf{c}_1^{\mathrm{H}}\mathbf{d}_2 \\ &\quad + \underbrace{\mathbf{c}_1^{\mathrm{H}}(\mathbf{h} \circ \mathbf{c}_3)}_{XT_{13}} \circ \mathbf{c}_1^{\mathrm{H}}\mathbf{d}_3 + \underbrace{\mathbf{c}_1^{\mathrm{H}}(\mathbf{h} \circ \mathbf{c}_4)}_{XT_{14}} \circ \mathbf{c}_1^{\mathrm{H}}\mathbf{d}_4 + \underbrace{\mathbf{c}_1^{\mathrm{H}}\mathbf{n}}_{n_1} \end{aligned} \tag{8}$$

Similarly, the receive beams for the other three codes are given as,

$$\begin{aligned} y_2 &= \underbrace{\mathbf{c}_2^{\mathrm{H}}(\mathbf{h} \circ \mathbf{c}_1)}_{XT_{21}} \circ \mathbf{c}_2^{\mathrm{H}}\mathbf{d}_1 + \underbrace{\mathbf{c}_2^{\mathrm{H}}(\mathbf{h} \circ \mathbf{c}_2)}_{B} \circ \mathbf{c}_2^{\mathrm{H}}\mathbf{d}_2 \\ &\quad + \underbrace{\mathbf{c}_2^{\mathrm{H}}(\mathbf{h} \circ \mathbf{c}_3)}_{XT_{23}} \circ \mathbf{c}_2^{\mathrm{H}}\mathbf{d}_3 + \underbrace{\mathbf{c}_2^{\mathrm{H}}(\mathbf{h} \circ \mathbf{c}_4)}_{XT_{24}} \circ \mathbf{c}_2^{\mathrm{H}}\mathbf{d}_4 + \underbrace{\mathbf{c}_2^{\mathrm{H}}\mathbf{n}}_{n_2} \end{aligned} \tag{9}$$

$$\begin{aligned} y_3 &= \underbrace{\mathbf{c}_3^{\mathrm{H}}(\mathbf{h} \circ \mathbf{c}_1)}_{XT_{31}} \circ \mathbf{c}_3^{\mathrm{H}}\mathbf{d}_1 + \underbrace{\mathbf{c}_3^{\mathrm{H}}(\mathbf{h} \circ \mathbf{c}_2)}_{XT_{32}} \circ \mathbf{c}_3^{\mathrm{H}}\mathbf{d}_2 \\ &\quad + \underbrace{\mathbf{c}_3^{\mathrm{H}}(\mathbf{h} \circ \mathbf{c}_3)}_{C} \circ \mathbf{c}_3^{\mathrm{H}}\mathbf{d}_3 + \underbrace{\mathbf{c}_3^{\mathrm{H}}(\mathbf{h} \circ \mathbf{c}_4)}_{XT_{34}} \circ \mathbf{c}_3^{\mathrm{H}}\mathbf{d}_4 + \underbrace{\mathbf{c}_3^{\mathrm{H}}\mathbf{n}}_{n_3} \end{aligned} \tag{10}$$

$$\begin{aligned} y_4 &= \underbrace{\mathbf{c}_4^{\mathrm{H}}(\mathbf{h} \circ \mathbf{c}_1)}_{XT_{41}} \circ \mathbf{c}_4^{\mathrm{H}}\mathbf{d}_1 + \underbrace{\mathbf{c}_4^{\mathrm{H}}(\mathbf{h} \circ \mathbf{c}_2)}_{XT_{42}} \circ \mathbf{c}_4^{\mathrm{H}}\mathbf{d}_2 \\ &\quad + \underbrace{\mathbf{c}_4^{\mathrm{H}}(\mathbf{h} \circ \mathbf{c}_3)}_{XT_{43}} \circ \mathbf{c}_4^{\mathrm{H}}\mathbf{d}_3 + \underbrace{\mathbf{c}_4^{\mathrm{H}}(\mathbf{h} \circ \mathbf{c}_4)}_{D} \circ \mathbf{c}_4^{\mathrm{H}}\mathbf{d}_4 + \underbrace{\mathbf{c}_4^{\mathrm{H}}\mathbf{n}}_{n_4} \end{aligned} \tag{11}$$

where A, B, C and D are the desired signal parts and now each code has cross-talk from the other three codes. Once again, the sum cross-talks at the UE, can be calculated as the channel $\mathbf{h}$ is known at the UE receiver. If the cross-talk is low, we can formulate a system of linear equations,

$$\begin{bmatrix} y_1 \\ y_2 \\ y_3 \\ y_4 \end{bmatrix} = \begin{bmatrix} A & XT_{12} & XT_{13} & XT_{14} \\ XT_{21} & B & XT_{23} & XT_{24} \\ XT_{31} & XT_{32} & C & XT_{34} \\ XT_{41} & XT_{42} & XT_{43} & D \end{bmatrix} \begin{bmatrix} d_1 \\ d_2 \\ d_3 \\ d_4 \end{bmatrix} + \begin{bmatrix} n_1 \\ n_2 \\ n_3 \\ n_4 \end{bmatrix} \tag{12}$$

which can be solved for the desired data symbols as,

$$\begin{aligned} \begin{bmatrix} d_1 \\ d_2 \\ d_3 \\ d_4 \end{bmatrix} &= \begin{bmatrix} A & XT_{12} & XT_{13} & XT_{14} \\ XT_{21} & B & XT_{23} & XT_{24} \\ XT_{31} & XT_{32} & C & XT_{34} \\ XT_{41} & XT_{42} & XT_{43} & D \end{bmatrix}^{-1} \begin{bmatrix} y_1 \\ y_2 \\ y_3 \\ y_4 \end{bmatrix} \\ &\quad + \begin{bmatrix} A & XT_{12} & XT_{13} & XT_{14} \\ XT_{21} & B & XT_{23} & XT_{24} \\ XT_{31} & XT_{32} & C & XT_{34} \\ XT_{41} & XT_{42} & XT_{43} & D \end{bmatrix}^{-1} \begin{bmatrix} n_1 \\ n_2 \\ n_3 \\ n_4 \end{bmatrix}. \end{aligned} \tag{13}$$

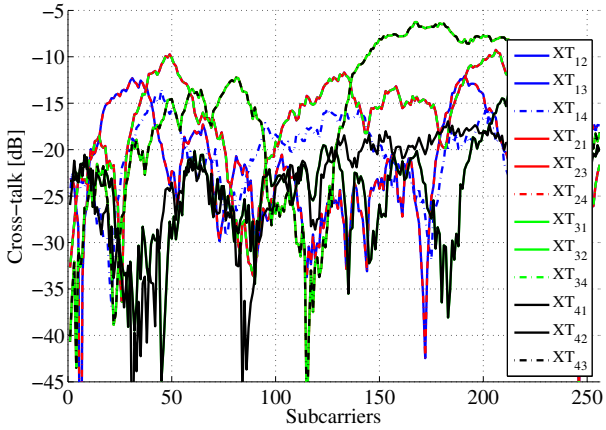

Fig. 4: Sum cross-talk over sub-carriers between 4 codes of length 32 for a measured channel.

Figure 4 shows the sum cross-talks for four coded multiplexed streams for an urban macro measured channel with noise. We can see a similar trend to the 2 code case where cross-talks below -20 dB can be achieved quite easily by properly adapting the beams to the subcarriers.

III. Orthogonally Coded Data Multiplexing over Combined Beams

A virtual antenna array of size 32, as evaluated above for a single antenna UE, would need the multiplexing of 32 data streams to achieve the same efficiency as a physical antenna array of the same size. Extension of coded data multiplexing from 4 parallel streams to up to 32 orthogonal streams is obviously challenging. In addition, beamforming SNR gains are lower or even zero for virtual compared to physical arrays, as the Tx power has to be shared between the codes. The user data transmission benefits therefore mainly from the improved

suppression of the interferer and the larger channel prediction horizon. Note, as CSI RSs do not have to share codes, but repeat the same signal multiple times, channel estimation itself profits also from SNR gains.

The above mentioned issues suggest to combine the benefits of two worlds and to enhance a limited set of physical UE antennas with virtual beamforming. For example, assuming an 8 antenna UE would require only 4 retransmissions to form a combined physical-virtual 32 element antenna array, which additionally can achieve a 9 dB SNR gain. In this case, full efficiency is already achieved by the multiplexing of 4 data streams over four orthogonal codes of length four transmitted in four time slots.

Instead of transmitting four streams to one UE, alternatively one might serve four streams to four different UEs, which would relax the fixed coupling of code and beamforming weights. In that case, the streams will be separated by MU-MIMO precoding instead of orthogonal Tx-codes. In practice, the number of active UEs might be often limited and a suitable mode adaptation might be needed.

In the following, we will investigate in more detail another potential setup, which combines low complexity with large virtual beamforming gains. It is based on the observation that the so far discussed 32 virtual antenna elements use a very low virtual antenna spacing of just 1 cm equal to 0.1λ for the given RF frequency of 2.6 GHz. The channel prediction quality is mainly affected by the half-power beamwidth (HPBW) of the virtual beamformer, which itself depends on the virtual antenna aperture. This is defined by the distance between the outer most antenna elements and will be unchanged by downsampling of antenna elements for example to a $\lambda/2$ spacing.

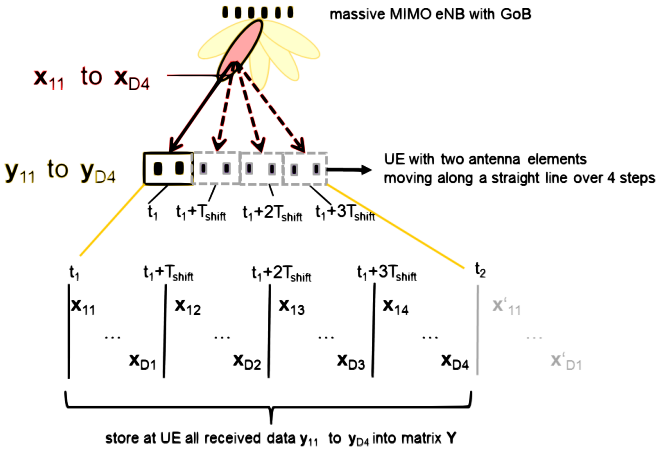

Fig. 5: Order of data transmission over one eNB beam to a combined 8 element antenna, consisting of 2 physical UE antennas and 4 virtual steps

An exemplary setup is given in Figure 5 for a 2 antenna element UE plus four virtual time steps forming a virtual eight element array with $\lambda/2 = 0.06$ m spacing. The figure additionally illustrates the overall timing diagram of the proposed concept. At a certain time instant t_1, the eNB transmits, for example, over one beam of a fixed grid-of-beam (GoB) the signal,

$$x_{11} = [\mathbf{c}_1(1)\ \mathbf{c}_2(1)\ \mathbf{c}_3(1)\ \mathbf{c}_4(1)][\mathbf{d}_1^1(t_1)\mathbf{d}_2^1(t_1)\mathbf{d}_3^1(t_1)\mathbf{d}_4^1(t_1)]^{\mathrm{T}} \tag{14}$$

leading to the receive vector,

$$\mathbf{y}_{11}(t_1) = [h_1(t_1)x_{11} \quad h_2(t_1)x_{11}]^{\mathrm{T}} + \mathbf{n}(t_1). \tag{15}$$

The second subscript j of the complex scalar Tx-signal x_{ij} is related to the time instant when it will be transmitted, i.e., $t = t_1$, $t_1 + T_{\text{shift}}$, $t_1 + 2T_{\text{shift}}$ and $t_1 + 3T_{\text{shift}}$. The first subscript i in x_{ij} corresponds to the superscript in the Tx symbols $\mathbf{d}_1^i$ to $\mathbf{d}_4^i$. It indicates the selected data symbols from the block of data for the parallel data streams $\mathbf{d}_1$ to $\mathbf{d}_4$. The length of the data blocks is given by the index D and has to be adapted to the time T_{shift} and the symbol timing so that a continuous data transmission can be achieved. Correspondingly, the transmission of $x_{(i+1)j}$ compared to x_{ij} is shifted by one symbol timing t_{symbol}.

For the given example, the UE receives x_{ij} with two Rx-antennas leading to the receive vector $\mathbf{y}_{ij}(t_k)$; $k = t_1, t_1 + T_{\text{shift}}, t_1 + 2T_{\text{shift}}, t_1 + 3T_{\text{shift}}$, where x_{ij} is affected by the corresponding channel coefficients for the different antenna elements and the Rx noise vector $\mathbf{n}$. The UE stores all Rx vectors $\mathbf{y}_{ij}(t_k)$ into the matrix $\mathbf{Y}$ to apply after full reception, the combined beamformers to all data sets.

Let us assume a UE moving with a speed of 43 km/h then one has to set T_{shift} to a value of 10 ms to achieve a λ spacing between two transmission steps, or equivalently, the $\lambda/2$ spaced combined virtual antenna array of Figure 5. For this scheme, the HPBW would be just 6 degrees compared to 17 degrees for the 32 element virtual antenna array.

IV. Conclusions

Virtual beamforming improves the performance of channel estimation and prediction significantly, but an overall 5G concept requires the inclusion of an efficient user data transmission. In this paper, we propose coded multiplexing of user data over virtual beams, which poses some novel challenges due to the tight code to beam shape interdependency. In addition, CSI knowledge at the eNB is limited to the virtually beamformed channel components so that the transmitter has no information about the channel induced code crosstalk at the receiver. In contrast, the UE can estimate the code crosstalk based on its full CSI knowledge and might easily cancel it by solving a known linear equation.

From a more general point of view, user data multiplexing over virtually beamformed antenna arrays will enhance 5G UE capabilities to form, e.g., strong IRC receivers, reduce the number of MPCs per relevant channel component and/or the number of relevant channel components itself. For a given limited set of physical antenna elements, the effective spatial degrees of freedom for the combined physical plus virtual ones might be significantly increased with moderate further hardware requirements.

ACKNOWLEDGMENT

This work has been performed in the framework of the Horizon 2020 project FANTASTIC-5G (ICT-671660) receiving funds from the European Union. The authors would like to acknowledge the contributions of their colleagues in the project, although the views expressed in this contribution are those of the authors and do not necessarily represent the project.

REFERENCES

[1] E. G. Larsson, F. Tufvesson, O. Edfors, and T. L. Marzetta, "Massive MIMO for next generation wireless systems," *IEEE Communications Magazine*, vol. 52, no. 2, pp. 186–195, 2013.

[2] S. Dierks, M. B. Amin, W. Zirwas, M. Haardt, and B. Panzner, "The benefit of cooperation in the context of massive MIMO," in *Proceedings of 18th International OFDM Workshop 2014 (InOWo'14)*, Aug 2014, pp. 1–8.

[3] V. D'Amico, "ARTIST4G Deliverable D1.4 - Interference avoidance techniques and system design," ARTIST4G consortium, http://publications.lib.chalmers.se/records/fulltext/212923/local_212923.pdf, Tech. Rep., July. 2012.

[4] M. B. Amin, W. Zirwas, and M. Haardt, "Design options in the context of 5G for a powerful channel prediction," in *Proceedings of the 35th Wireless World Research Forum (WWRF 35)*, 2015.

[5] K. T. Truong and R. W. H. Jr., "Effects of channel aging in massive MIMO systems," *CoRR*, vol. abs/1305.6151, 2013.

[6] R. Apelfrojd and M. Sternad, "Design and measurement-based evaluations of coherent JT CoMP: a study of precoding, user grouping and resource allocation using predicted CSI," *EURASIP Journal on Wireless Communications and Networking*, 2014.

[7] D. Aronsson, "Channel estimation and prediction for MIMO OFDM systems: Key design and performance aspects of kalman based algorithms," Ph.D. dissertation, Uppsala University, Sweden, 2011.

[8] M. Milojevic, G. Del Galdo, and M. Haardt, "Tensor-based framework for the prediction of frequency-selective time-variant MIMO channels," in *Proceedings of International ITG Workshop on Smart Antennas (WSA 2008)*, 2008.

[9] M. B. Amin, W. Zirwas, and M. Haardt, "Advanced channel prediction concepts for 5G radio systems," in *Proceedings of the Twelfth International Symposium on Wireless Communication Systems (ISWCS 15)*, 2015.

[10] P. Baracca and D. Aziz, "METIS deliverable 3.4," The METIS 2020 Project, https://www.metis2020.com/wp-content/uploads/deliverables/METIS_D3.3_v1.pdf, Tech. Rep., 2015.

[11] W. Zirwas and M. Haardt, "Channel prediction for B4G radio systems," in *Proceedings of 77th IEEE Vehicular Technology Conf. (VTC 2013 Spring)*, 2013.